

Exfoliated hexagonal BN as gate dielectric for InSb nanowire quantum dots with improved gate hysteresis and charge noise

Felix Jekat,¹ Benjamin Pestka,¹ Diana Car,² Saša Gazibegović,² Kilian Flöhr,¹ Sebastian Heedt,^{3, a)} Jürgen Schubert,³ Marcus Liebmann,¹ Erik P. A. M. Bakkers,² Thomas Schäpers,³ and Markus Morgenstern^{1, b)}

¹⁾*II. Institute of Physics B, RWTH Aachen University and JARA-FIT, 52074 Aachen, Germany*

²⁾*Department of Applied Physics, Eindhoven University of Technology, 5600 MB Eindhoven, The Netherlands*

³⁾*Peter Grünberg Institut (PGI-9) and JARA-FIT, Forschungszentrum Jülich, 52425 Jülich, Germany*

(Dated: November 2, 2022)

We characterize InSb quantum dots induced by bottom finger gates within a nanowire that is grown via the vapor-liquid-solid process. The gates are separated from the nanowire by an exfoliated 35 nm thin hexagonal BN flake. We probe the Coulomb diamonds of the gate induced quantum dot exhibiting charging energies of ~ 2.5 meV and orbital excitation energies up to 0.3 meV. The gate hysteresis for sweeps covering 5 Coulomb diamonds reveals an energy hysteresis of only 60 μ eV between upwards and downwards sweeps. Charge noise is studied via long-term measurements at the slope of a Coulomb peak revealing potential fluctuations of ~ 1 μ eV/ $\sqrt{\text{Hz}}$ at 1 Hz. This makes h-BN the dielectric with the currently lowest gate hysteresis and lowest low-frequency potential fluctuations reported for low-gap III-V nanowires. The extracted values are similar to state-of-the-art quantum dots within Si/SiGe and Si/SiO₂ systems.

Recently, nanowires of indium antimonide (InSb) and indium arsenide (InAs)^{1–4} came back into focus due to their large spin-orbit coupling^{5–7} that in combination with magnetic fields and a relatively strong proximity-induced superconductivity^{8–10} enables tuning of Majorana modes^{11–14} as a basis for topologically protected quantum computing.^{15–17} Typically, the nanowires are tuned electrically by a number of bottom finger gates that are separated from the nanowire by a gate dielectric.^{12,18} It is well known that both charge noise and hysteresis of gate-induced potentials deteriorate the performance of semiconductor qubits,^{19–22} as is also expected for the prospective Majorana qubits.^{23,24} Hence, it is crucial to optimize the dielectric in terms of unintentional charge fluctuations.

For exfoliated two-dimensional materials such as graphene, it turned out that hexagonal boron nitride (h-BN) is ideal for that purpose.^{25,26} For example, it improves the charge carrier mobility by more than an order of magnitude compared to the previously used Si/SiO₂.^{27,28} Furthermore, it is easy to fabricate. Thus, exploiting exfoliated h-BN as gate dielectric for low-gap III-V nanowires is appealing. First experiments used h-BN to separate the global Si/SiO₂ back gate from an InSb nanowire enabling the first quantized conductance steps in such nanowires at zero magnetic field.²⁹ Subsequently, measurements on proximity-coupled InSb nanowires on h-BN showed magnetic field induced zero bias peaks, indicative of the presence of Majorana zero modes.^{30,31} However, Coulomb diamonds (CDs) with excited states in a gate-induced quantum dot (QD) have not been reported and, more importantly, the charge noise and gate hysteresis of such nanowires on h-BN have not been studied. Reports on these properties are only available for other types of dielectrics.^{32–42} They ex-

hibit, e.g., a relatively large low-temperature gate hysteresis on LaLuO₃ and SiO₂ being 0.5 V and 2 V at gate sweep ranges of 4 V and 30 V, respectively.^{41,42} Noise properties for QDs have only been reported for a vacuum dielectric revealing $1/f$ behavior above ~ 300 Hz and an upturn at lower frequency with noise of ~ 0.2 μ eV/ $\sqrt{\text{Hz}}$ at 100 Hz.³³

Here, we study an InSb nanowire/h-BN device with bottom finger gates (pitch 90 nm) at the temperature $T = 300$ mK. The device exhibits a gate hysteresis of 2 mV for sweeps of 150 mV (250 mV) at a rate of 25 mV/s (42 mV/h), hence, significantly better than in previous reports.^{41,42} It, moreover, shows a charge noise of only 1 μ eV/ $\sqrt{\text{Hz}}$ at 1 Hz with an approximate $1/f^{1.5}$ dependence towards lower frequencies. The noise is similar to the previously studied vacuum dielectric³³ pointing to remaining limitations due to defects at the nanowire itself. More importantly, the value is slightly better than for state-of-the-art QDs in Si/SiGe or Si/SiO₂ structures (~ 3 μ eV/ $\sqrt{\text{Hz}}$ at 1 Hz).^{22,43–45} Hence, h-BN turns out to be a favorable dielectric for low-gap III-V nanowires.

The InSb nanowires were grown on top of InP stems via the vapor-liquid-solid (VLS) method using a gold droplet as catalyst.^{46,47} A QD device of such a nanowire (Fig. 1(a)–(b)) consists of a 200 nm thick SiN_x layer, on a highly doped Si substrate acting as a global back gate (BG) with multiple finger gates (G1–G4, FG) on top. The finger gates are 35 nm wide and defined by electron beam lithography (EBL) with a spacing of 55 nm except between G3 and FG where the spacing is 130 nm. An h-BN flake is deposited on top of the finger gates via the dry transfer method.²⁷ Subsequently, one InSb nanowire is placed onto the h-BN with sub- μ m lateral precision via an indium tip attached to a micromanipulator.⁴⁸ Finally, source and drain contacts are prepared via EBL. Prior to the metal deposition of the Ti/Au (10 nm/110 nm) contacts, the exposed nanowire area is passivated ex-situ by sulphur⁴⁹ and subsequently cleaned in-situ by argon ion bombardment. Transport measurements are performed at $T = 300$ mK in a ³He magneto-cryostat (Teslatron from Oxford Instruments).

^{a)}Current address: Microsoft Quantum Lab Delft, 2600 GA Delft, The Netherlands

^{b)}mmorgens@physik.rwth-aachen.de

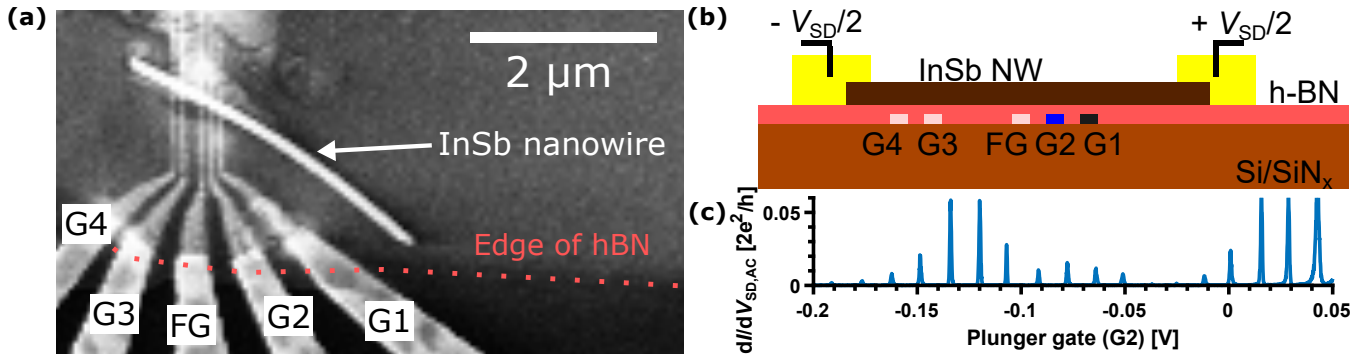


Figure 1. (a) Scanning electron microscopy image of the device prior to depositing source and drain contacts. Different finger gates (G1-G4) and a floating gate (FG) are labeled. Nanowire diameter: ~ 100 nm. (b) Side view sketch of the device. Si/SiN_x (light brown) acts as a global backgate (BG). Finger gates G1-G4 and FG (white, blue, black) are deposited on top and buried below a 35 nm thick h-BN flake (pink). The nanowire (dark brown) is contacted by two Ti/Au pads (yellow) at distance 2.2 μm used to apply the source-drain voltage V_{SD} . Light brown, blue and black colors of gates match the colors of the corresponding phase stability diagrams in Fig. 2, where these gates are used as plunger gate. (c) Nanowire conductance $dI/dV_{SD,AC}$ as a function of plunger gate voltage V_{G2} at gate G2. Coulomb peaks appear due to the formation of a QD confined by energy barriers that are induced via G1 and G3, $V_{G1} = -970$ mV, $V_{G3} = -463$ mV, $V_{BG} = 3$ V, $V_{SD,AC} = 20$ μV, $f_{AC} = 933.5$ Hz, $V_{SD,DC} = 0$ V, $T = 300$ mK.

Before cool-down, the insert is evacuated to 10^{-6} mbar for 48 h at 300 K in order to remove adsorbates from the nanowire surface.⁴²

Gate dependent conductivity traces (not shown) reveal a low temperature mobility of the nanowire of $\mu = 28000$ cm²/Vs.⁴² Using the finger gates, we induce a QD within the nanowire exhibiting regularly spaced Coulomb peaks of different heights (Fig. 1(c)), probably due to different coupling of the states to the tunnel barriers. Different combinations of finger gates reveal charge stability diagrams of such QDs with regularly spaced CDs for all combinations of gates and excited states at larger V_{SD} (Fig. 2(a)-(c)). Only very few perturbations appear, likely caused by uncontrolled charging events in the surrounding of the QD. We could not measure the last CD prior to depletion probably due to the elongated QD geometry decoupling the lowest energy state from the tunnel barriers. For the CDs of Fig. 2(a)-(c), one straightforwardly deduces charging energies E_C up to 3 meV, 2.3 meV, and 2.5 meV and lever arms α of 0.05 eV/V, 0.12 eV/V, and 0.03 eV/V, respectively. Estimating the QD extension via the QD capacitance $C = e^2/E_C = 70$ aF assuming, for the sake of simplicity, charging of an isolated sphere of radius r , we reasonably find $2r = 2 \frac{C}{4\pi\epsilon_0\epsilon_r} = 74$ nm⁵⁰ using the dielectric constant of InSb $\epsilon_r = 16.8$. The deduced diameter $2r$ is a bit smaller than gate spacing and nanowire diameter (~ 100 nm). This could partly be due to squeezing of the QD area in the direction perpendicular to the wire axis via the gate voltages as indeed found by COMSOL[®] simulations.⁵¹

To quantify the charge noise acting on the nanowire QDs, Fig. 3(a) shows low-frequency noise measurements for the three different gate configurations. We measure the temporal current fluctuations $\delta I(t)$ at the slope of a Coulomb peak for $V_{SD,AC} = 20$ μV. In order to transfer this to the potential fluctuation noise $S_{pot}(f)$ as function of frequency f , we firstly use the measured shape of the Coulomb peak in $I(V_{Gate})$ traces, well fitted by a Fermi-Dirac peak, to deduce the gate voltage

variation, $\delta V_{Gate}(t)$. Then, we transfer $\delta V_{Gate}(t)$ to potential energy variation $\delta E(t) = \alpha \delta V_{Gate}(t)$ with α as deduced from respective CDs. The square root of the single-sided power spectral density of the resulting $\delta E(t)$ in the QD leads to $S_{pot}(f)$ in eV/ $\sqrt{\text{Hz}}$ as displayed in Fig. 3(a) with the rms potential noise being $\delta E_{rms}^2 = \int S_{pot}^2(f) df$ across the measurement bandwidth. We find $S_{pot}(1 \text{ Hz}) = 1$ μeV/ $\sqrt{\text{Hz}}$ and an increase towards lower f mostly following $S_{pot}^2(f) \propto 1/f^{1.5}$ (red fit line). The enhanced logarithmic slope of $S_{pot}^2(f)$ with respect to the classical $1/f$ noise is in reasonable agreement with the upturn of the $1/f$ noise below $f = 100$ Hz observed earlier for InAs nanowires with vacuum dielectric.³³

We also display a direct comparison of quantum point contacts (QPCs) for the InSb nanowire on hBN with an InAs nanowire⁵² on a LaLuO₃ dielectric. Except for the dielectric, deposited via pulsed laser deposition⁴¹, the two devices are prepared identically. The QPC is formed by charging one of the finger gates only with all other gates grounded. The displayed $S_{pot}(f)$ (Fig. 3(a), orange) originates from $\delta I(t)$ at the pinch-off of the nanowire induced by a single finger gate. It is converted to $S_{pot}(f)$ by the measured $I(V_{Gate})$ using $\alpha_{hBN} = 0.12 \pm 0.02$ eV/V for the hBN device as determined from the corresponding QD CDs with error bars as deduced from CD variations and $\alpha_{LaLuO_3} = 0.55 \pm 0.11$ eV/V for the LaLuO₃ device deduced by scaling α_{hBN} for the different thicknesses (hBN: 35 ± 2 nm, LaLuO₃: 50 ± 5 nm) and for the different ϵ (hBN: $\simeq 4$ ⁵³, LaLuO₃: 26 ± 1 ⁵⁴). Remarkably, $S_{pot}(f)$ of the h-BN device is more than two orders of magnitude lower than for the LaLuO₃ device (Fig. 3(a)) illustrating the excellent properties of the hBN dielectric. We employed all four finger gates for such QPC measurements. The resulting $S_{pot}(f)$ curves are nearly identical up to 1 Hz, but vary at higher frequency being either lower by up to a factor of four or larger by up to a factor of three with respect to the displayed curve. This indicates the presence of particular fluctuators at ~ 10 Hz in the device^{45,55}.

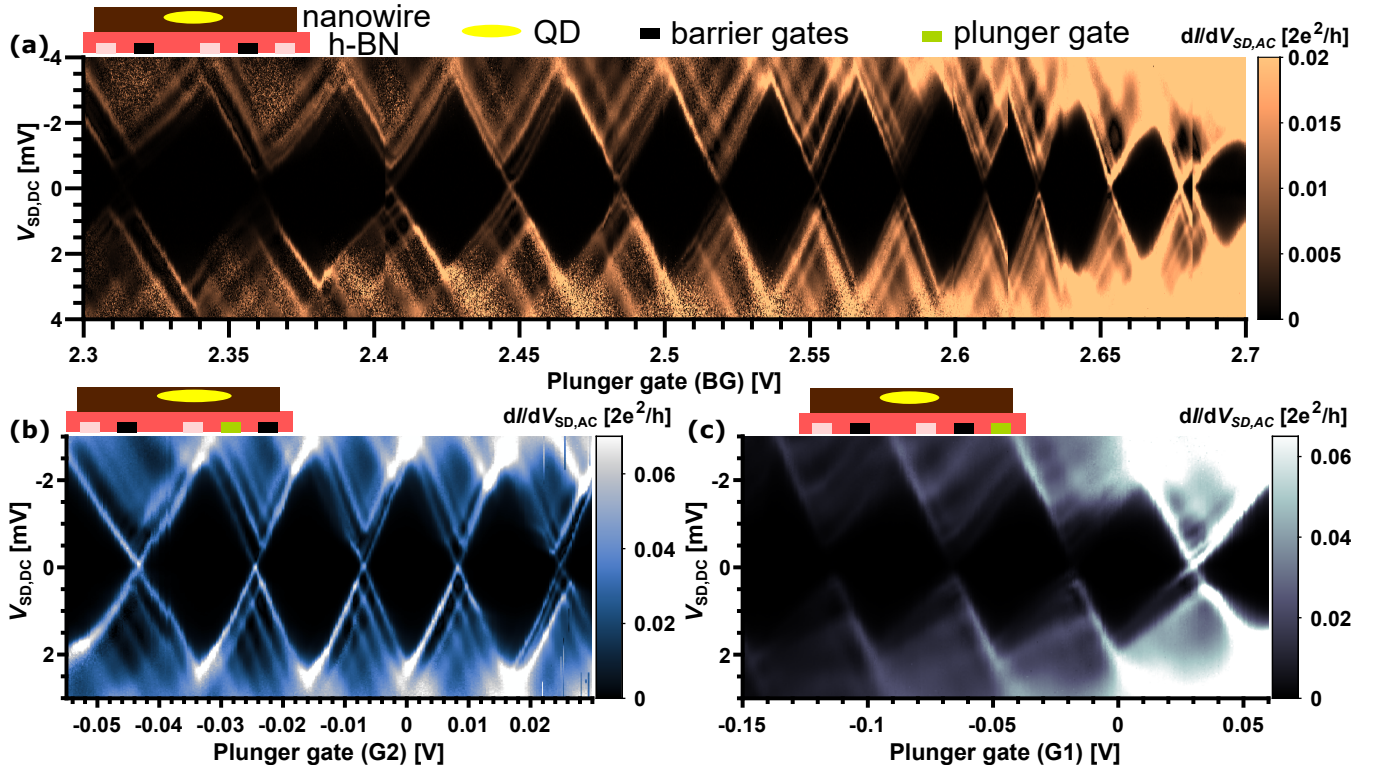


Figure 2. Charge stability diagrams of different QDs in the same InSb nanowire using different combinations of finger gates as sketched on top including the resulting QD area (yellow). Fast scan direction is along $V_{SD,DC}$, $V_{SD,AC} = 20 \mu\text{V}$, $f_{AC} = 83 \text{ Hz}$, $V_{G4} = 0 \text{ V}$, $T = 300 \text{ mK}$. (a) QD confined by G2 and G3 (black) and charged by the back gate (BG), $V_{G2} = -700 \text{ mV}$, $V_{G3} = -1 \text{ V}$, $V_{G1} = 0 \text{ V}$. A few perturbations are visible at $V_{BG} = 2.68 \text{ V}$, 2.64 V , 2.62 V and 2.6 V , likely due to uncontrolled charging events during the early stages of the measurement. (b) QD confined by G1 and G3 (black) and charged by G2 (green), $V_{G1} = -650 \text{ mV}$, $V_{G3} = -980 \text{ mV}$, $V_{BG} = 3 \text{ V}$. (c) QD confined by G2 and G3 (black) and charged by G1 (green), $V_{G2} = -580 \text{ mV}$, $V_{G3} = -922 \text{ mV}$, $V_{BG} = 3 \text{ V}$.

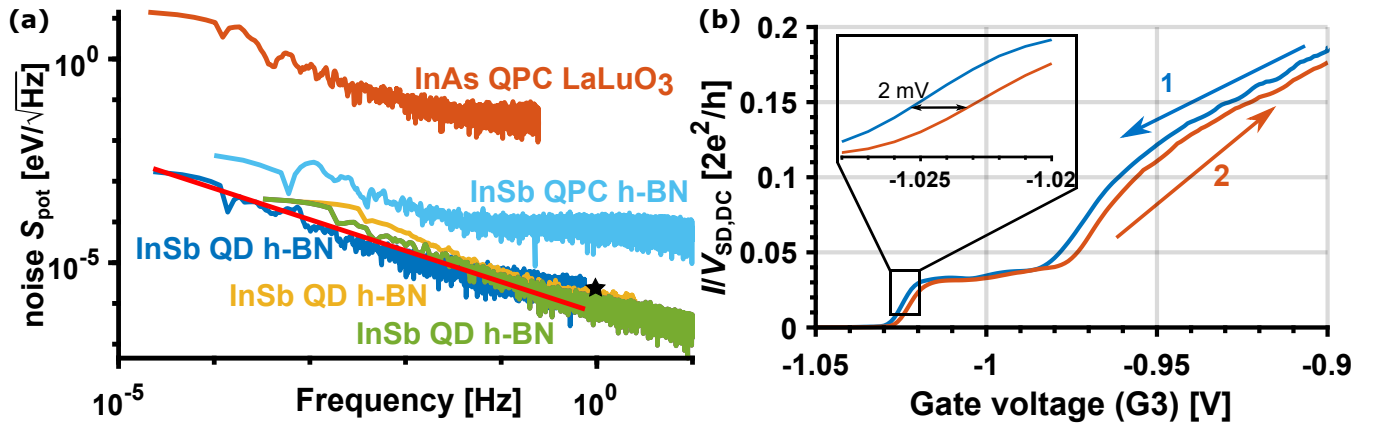


Figure 3. (a) Potential fluctuation noise $S_{\text{pot}}(f)$ as function of frequency f for several InSb nanowire QDs on h-BN using different gate configurations that yield $E_C = 3 \text{ meV}$ (blue), $E_C = 1.8 \text{ meV}$ (yellow), $E_C = 1 \text{ meV}$ (green) with fit curve $S_{\text{pot}}^2(f) \propto 1/f^{1.5}$ (red). The black star shows a benchmark $S_{\text{pot}}(f)$ for Si and Si/SiGe QDs^{43–45}. Additionally, $S_{\text{pot}}(f)$ for a QPC within the same InSb nanowire on h-BN (light blue, $V_{SD,DC} = 3 \text{ mV}$, $V_{SD,AC} = 20 \mu\text{V}$, $f_{AC} = 933.5 \text{ Hz}$, $V_{G3} = -600 \text{ mV}$, all other gates grounded) is compared to $S_{\text{pot}}(f)$ of a QPC within an InAs nanowire on LaLuO₃ (orange, $V_{SD,DC} = 5 \text{ mV}$, $V_{SD,AC} = 20 \mu\text{V}$, $f_{AC} = 1.1 \text{ kHz}$, $V_{G1} = -10 \text{ V}$, all other gates grounded). Both devices are fabricated using the same deposition methods except for the dielectric. The noise background as determined in the Coulomb blockade region of the QDs is more than a factor of 10 lower than all displayed $S_{\text{pot}}(f)$. (b) V_{G3} dependent conductance of the InSb nanowire on h-BN close to pinch-off (without inducing a QD). Arrows with numbers indicate the subsequent sweep directions of V_{G3} . Inset: zoom showing a hysteresis of $\sim 2 \text{ mV}$, sweep rate: 25 mV/s , $V_{SD,DC} = 3 \text{ mV}$, $V_{SD,AC} = 20 \mu\text{V}$, $f_{AC} = 83 \text{ Hz}$, $V_{BG} = 3 \text{ V}$, all other gates grounded. (a), (b) $T = 300 \text{ mK}$.

Comparison with literature data on noise for III-V low-gap nanowires is difficult. Either much longer parts of the nanowire are gated³², effectively averaging charge fluctuations, or the frequencies are larger due to probing by radio frequency via reflection at the QD.³³ Extrapolating the latter noise data obtained for a suspended InAs nanowire (vacuum dielectric) at 100 Hz³³ towards 10 Hz via the measured $1/f^{1.5}$ dependence leads to $S_{\text{pot}}(10 \text{ Hz}) \simeq 1 \mu\text{eV}/\sqrt{\text{Hz}}$, larger than for our device on h-BN ($0.4 \mu\text{eV}/\sqrt{\text{Hz}}$ at 10 Hz). However, the data with vacuum dielectric are measured at 1.5 K such that extrapolating to 0.3 K by the established linear temperature dependence^{44,45} yields $S_{\text{pot}}(10 \text{ Hz}, 0.3 \text{ K}) \simeq 0.2 \mu\text{eV}/\sqrt{\text{Hz}}$, slightly better but still rather similar to our device. Since vacuum exhibits no defects acting as charge traps, Nilson et al.³³ conjectured that the major charge noise originates from charge traps within or on the nanowire and not from the dielectric. Regarding the similarity of $S_{\text{pot}}(10 \text{ Hz}, 0.3 \text{ K})$, we believe that this is correct for our device, too.

It is instructive to compare our data with the charge noise in Si or Si/SiGe QDs^{22,43–45,55}, currently considered as most promising for semiconductor spin qubits⁵⁶. For these QDs, one finds $S_{\text{pot}}^2(f \simeq 1 \text{ Hz}) \propto 1/f^\beta$ with device-dependent $\beta = 1 - 1.4$ and, consistently, an increase of $S_{\text{pot}}(f)$ with increasing T . Favorably, the reported $S_{\text{pot}}(f)$ at 0.3 K ($1-5 \mu\text{eV}/\sqrt{\text{Hz}}$ at 1 Hz)^{43–45,55} (star in Fig. 3(a)) is not smaller than for our InSb nanowire QD on h-BN ($\sim 1 \mu\text{eV}/\sqrt{\text{Hz}}$ at 1 Hz). This renders the device competitive to the most favorable material combinations in terms of charge noise.

The second important benchmark for a dielectric is the gate hysteresis. Figure 3(b) reveals that the InSb nanowire on h-BN exhibits a gate hysteresis $\Delta V_{\text{hyst}} \simeq 2 \text{ mV}$ (inset) at a sweep rate of 25 mV/s. Since it is known that the hysteresis strongly depends on the probed gate range, we scale the hysteresis by the gate range for comparison. For the gate range $\Delta V_{\text{gate}} = 150 \text{ mV}$, this leads to a ratio $R = \Delta V_{\text{hyst}}/\Delta V_{\text{gate}} = 0.013$. This is much lower than observed previously for InAs or InSb nanowires on other gate dielectrics: $R = 0.13$ ⁴¹, $R = 0.07$ ⁴², where higher temperatures (25 K, 4.2 K) have been employed that typically even reduce hysteresis as indeed found in one of these studies⁴¹. Since R additionally depends on the sweep rate^{57,58}, we improved it further by reducing the gate sweep rate to 42 mV/h leading to $R = 0.008$ with $\Delta V_{\text{gate}} = 250 \text{ mV}$. The extremely low rate is employed to record full charge stability diagrams subsequently for both gate sweep directions (Fig. 4(a),(b)). The total measurement time of 12 h evidences the long term stability of the QD by the excellent similarity of the two diagrams. Only two conductivity jumps (Fig. 4(b), right) are observed. The gate hysteresis is quantified by a line cut at $V_{\text{SD}} = 0 \text{ mV}$ (Fig. 4(c)) revealing $\Delta V_{\text{hyst}} = 2 \text{ mV}$ as maximum hysteresis between the two curves (inset) and, hence, implying $R = 0.008$. Using $\alpha = 0.03 \text{ eV/V}$, one can calculate the energy hysteresis $\Delta E = 60 \mu\text{eV}$. Figure 4(d) displays the difference between Fig. 4(b) and Fig. 4(a) showing that the small hysteresis is reliably observed across the whole charge stability diagram. The observation of a small hysteresis, low charge noise and a small number of jumps in stability diagrams consistently indicate a very low number of chargeable

impurities in the h-BN layer, thus making it a favorable dielectric for III-V nanowire devices. As pointed out above, the performance is likely limited by the remaining charge traps on the nanowire itself.

In summary, we have presented an InSb nanowire device with an h-BN flake as gate dielectric. With a set of finger gates, electrons are confined in QDs using different gate configurations, resulting in regular Coulomb diamonds with multiple excited states. Favorably, the device has the lowest noise level ($1 \mu\text{eV}/\sqrt{\text{Hz}}$ at $\sim 1 \text{ Hz}$) reported for low-gap III-V nanowire devices yet and shows an unprecedented gate hysteresis of 2 mV only. Hence, in terms of charge noise, h-BN is the currently most favorable dielectric for low-gap III-V nanowire devices.

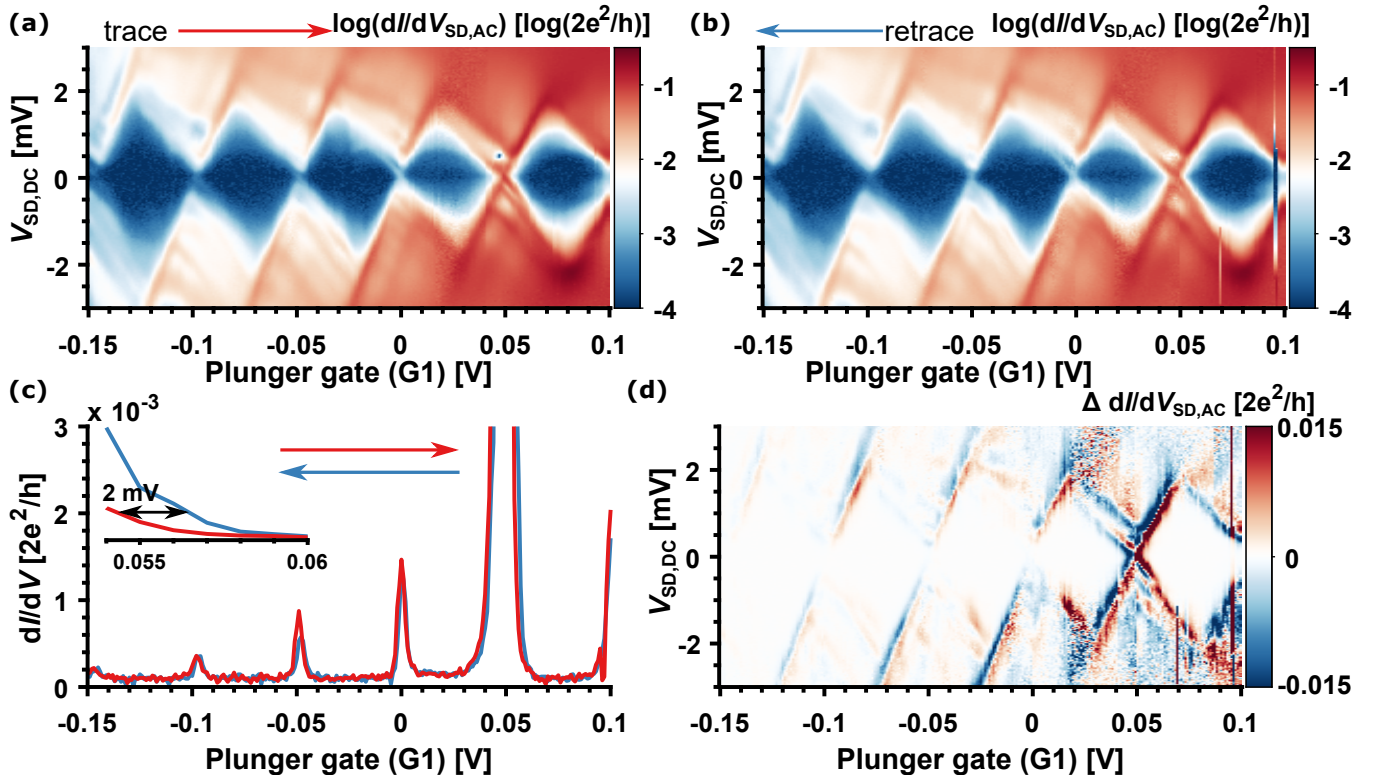


Figure 4. (a), (b) Charge stability diagrams for a QD confined by gates G2 and G3 and charged by gate G1. The two diagrams are recorded directly after each other with different gate sweep directions as marked by arrows on top. Fast sweep direction is along $V_{SD,DC}$, total measurement time: 12 h, gate sweep rate: 42 mV/h. (c) Line cut through (a) (red) and (b) (blue) at $V_{SD,DC} = 0$ mV. Inset: zoom with marked hysteresis of 2 mV. (d) Difference of the data of (b) and (a). Parameters: $V_{G2} = -580$ mV, $V_{G3} = -922$ mV, $V_{BG} = 3$ V, $V_{SD,AC} = 20$ μ V, $f_{AC} = 83$ Hz, $T = 300$ mK.

ACKNOWLEDGMENTS

We thank Stefan Trelenkamp and Florian Lentz for help with the EBL and acknowledge helpful discussions with Hendrik Bluhm. Funding by the Deutsche Forschungsgemeinschaft (DFG, German Research Foundation) under Germany's Excellence Strategy – Cluster of Excellence Matter and Light for Quantum Computing (ML4Q) EXC 2004/1 – 390534769 and by European Graphene Flagship Core 2, grant number 785219 is gratefully acknowledged.

REFERENCES

- ¹K. Hiruma, M. Yazawa, T. Katsuyama, K. Ogawa, K. Haraguchi, M. Koguchi, and H. Kakibayashi, "Growth and optical properties of nanometer-scale GaAs and InAs whiskers," *J. Appl. Phys.* **77**, 447–462 (1995).
- ²L. E. Jensen, M. T. Björk, S. Jeppesen, A. I. Persson, B. J. Ohlsson, and L. Samuelson, "Role of surface diffusion in chemical beam epitaxy of InAs nanowires," *Nano Lett.* **4**, 1961–1964 (2004).
- ³M. T. Björk, B. J. Ohlsson, C. Thelander, A. I. Persson, K. Deppert, L. R. Wallenberg, and L. Samuelson, "Nanowire resonant tunneling diodes," *Appl. Phys. Lett.* **81**, 4458–4460 (2002).
- ⁴B. M. Borg and L.-E. Wernersson, "Synthesis and properties of antimonide nanowires," *Nanotechnology* **24**, 202001 (2013).
- ⁵H. A. Nilsson, P. Caroff, C. Thelander, M. Larsson, J. B. Wagner, L.-E. Wernersson, L. Samuelson, and H. Q. Xu, "Giant, level-Dependent Factors in InSb nanowire quantum dots," *Nano Lett.* **9**, 3151–3156 (2009).
- ⁶S. Nadj-Perge, S. M. Frolov, E. P. A. M. Bakkers, and L. P. Kouwenhoven, "Spin-orbit qubit in a semiconductor nanowire," *Nature* **468**, 1084–1087 (2010).
- ⁷C. Fasth, A. Fuhrer, L. Samuelson, V. N. Golovach, and D. Loss, "Direct measurement of the spin-orbit interaction in a two-electron InAs nanowire quantum dot," *Phys. Rev. Lett.* **98**, 266801 (2007).
- ⁸Y.-J. Doh, "Tunable supercurrent through semiconductor nanowires," *Science* **309**, 272–275 (2005).
- ⁹H. Takayanagi and T. Kawakami, "Superconducting proximity effect in the native inversion layer on InAs," *Phys. Rev. Lett.* **54**, 2449–2452 (1985).
- ¹⁰H. A. Nilsson, P. Samuelsson, P. Caroff, and H. Q. Xu, "Supercurrent and multiple andreev reflections in an InSb nanowire josephson junction," *Nano Lett.* **12**, 228–233 (2012).
- ¹¹J. Alicea, "New directions in the pursuit of majorana fermions in solid state systems," *Rep. Prog. Phys.* **75**, 076501 (2012).
- ¹²V. Mourik, K. Zuo, S. M. Frolov, S. R. Plissard, E. P. A. M. Bakkers, and L. P. Kouwenhoven, "Signatures of majorana fermions in hybrid superconductor-semiconductor nanowire devices," *Science* **336**, 1003–1007 (2012).
- ¹³S. M. Albrecht, A. P. Higginbotham, M. Madsen, F. Kuemmeth, T. S. Jespersen, J. Nygård, P. Krogstrup, and C. M. Marcus, "Exponential protection of zero modes in majorana islands," *Nature* **531**, 206–209 (2016).
- ¹⁴R. M. Lutchyn, E. P. A. M. Bakkers, L. P. Kouwenhoven, P. Krogstrup, C. M. Marcus, and Y. Oreg, "Majorana zero modes in superconductor-semiconductor heterostructures," *Nat. Rev. Mater.* **3**, 52–68 (2018).
- ¹⁵A. Stern and N. H. Lindner, "Topological quantum computation—from basic concepts to first experiments," *Science* **339**, 1179–1184 (2013).
- ¹⁶S. Vijay, T. H. Hsieh, and L. Fu, "Majorana fermion surface code for universal quantum computation," *Phys. Rev. X* **5**, 041038 (2015).

- ¹⁷D. Litinski, M. S. Kesselring, J. Eisert, and F. von Oppen, “Combining topological hardware and topological software: Color-code quantum computing with topological superconductor networks,” *Phys. Rev. X* **7**, 031048 (2017).
- ¹⁸A. Das, Y. Ronen, Y. Most, Y. Oreg, M. Heiblum, and H. Shtrikman, “Zero-bias peaks and splitting in an al-InAs nanowire topological superconductor as a signature of majorana fermions,” *Nat. Phys.* **8**, 887–895 (2012).
- ¹⁹D. Culcer, X. Hu, and S. D. Sarma, “Dephasing of si spin qubits due to charge noise,” *Appl. Phys. Lett.* **95**, 073102 (2009).
- ²⁰A. V. Kuhlmann, J. Houel, A. Ludwig, L. Greuter, D. Reuter, A. D. Wieck, M. Poggio, and R. J. Warburton, “Charge noise and spin noise in a semiconductor quantum device,” *Nat. Phys.* **9**, 570–575 (2013).
- ²¹J. Yoneda, K. Takeda, T. Otsuka, T. Nakajima, M. R. Delbecq, G. Allison, T. Honda, T. Koderu, S. Oda, Y. Hoshi, N. Usami, K. M. Itoh, and S. Tarucha, “A quantum-dot spin qubit with coherence limited by charge noise and fidelity higher than 99.9%,” *Nat. Nanotechnol.* **13**, 102–106 (2017).
- ²²X. Mi, S. Kohler, and J. R. Petta, “Landau-zener interferometry of valley-orbit states in si/SiGe double quantum dots,” *Phys. Rev. B* **98**, 161404 (2018).
- ²³M. J. Schmidt, D. Rainis, and D. Loss, “Decoherence of majorana qubits by noisy gates,” *Phys. Rev. B* **86**, 085414 (2012).
- ²⁴T. Li, W. A. Coish, M. Hell, K. Flensberg, and M. Leijnse, “Four-majorana qubit with charge readout: Dynamics and decoherence,” *Phys. Rev. B* **98**, 205403 (2018).
- ²⁵A. K. Geim and I. V. Grigorieva, “Van der waals heterostructures,” *Nature* **499**, 419–425 (2013).
- ²⁶R. Frisenda, E. Navarro-Moratalla, P. Gant, D. P. D. Lara, P. Jarillo-Herrero, R. V. Gorbachev, and A. Castellanos-Gomez, “Recent progress in the assembly of nanodevices and van der waals heterostructures by deterministic placement of 2d materials,” *Chem. Soc. Rev.* **47**, 53–68 (2018).
- ²⁷C. R. Dean, A. F. Young, I. Meric, C. Lee, L. Wang, S. Sorgenfrei, K. Watanabe, T. Taniguchi, P. Kim, K. L. Shepard, and J. Hone, “Boron nitride substrates for high-quality graphene electronics,” *Nat. Nanotechnol.* **5**, 722–726 (2010).
- ²⁸L. Banszerus, M. Schmitz, S. Engels, M. Goldsche, K. Watanabe, T. Taniguchi, B. Beschoten, and C. Stampfer, “Ballistic transport exceeding 28 μm in CVD grown graphene,” *Nano Lett.* **16**, 1387–1391 (2016).
- ²⁹J. Kammhuber, M. C. Cassidy, H. Zhang, Ö. Gül, F. Pei, M. W. A. de Moor, B. Nijholt, K. Watanabe, T. Taniguchi, D. Car, S. R. Plissard, E. P. A. M. Bakkers, and L. P. Kouwenhoven, “Conductance quantization at zero magnetic field in InSb nanowires,” *Nano Lett.* **16**, 3482–3486 (2016).
- ³⁰Ö. Gül, H. Zhang, J. D. S. Bommer, M. W. A. de Moor, D. Car, S. R. Plissard, E. P. A. M. Bakkers, A. Geresdi, K. Watanabe, T. Taniguchi, and L. P. Kouwenhoven, “Ballistic majorana nanowire devices,” *Nat. Nanotechnol.* **13**, 192–197 (2018).
- ³¹S. T. Gill, J. Damasco, B. E. Janicek, M. S. Durkin, V. Humbert, S. Gazibegovic, D. Car, E. P. A. M. Bakkers, P. Y. Huang, and N. Mason, “Selective-area superconductor epitaxy to ballistic semiconductor nanowires,” *Nano Lett.* **18**, 6121–6128 (2018).
- ³²M. R. Sakr and X. P. A. Gao, “Temperature dependence of the low frequency noise in indium arsenide nanowire transistors,” *Appl. Phys. Lett.* **93**, 203503 (2008).
- ³³H. A. Nilsson, T. Duty, S. Abay, C. Wilson, J. B. Wagner, C. Thelander, P. Delsing, and L. Samuelson, “A radio frequency single-electron transistor based on an InAs/InP heterostructure nanowire,” *Nano Lett.* **8**, 872–875 (2008).
- ³⁴C. J. Delker, S. Kim, M. Borg, L. Wernersson, and D. B. Janes, “1/f noise sources in dual-gated indium arsenide nanowire transistors,” *IEEE T. Electron. Dev.* **59**, 1980–1987 (2012).
- ³⁵S. Vitusevich and I. Zadorozhnyi, “Noise spectroscopy of nanowire structures: fundamental limits and application aspects,” *Semicond. Sci. Tech.* **32**, 043002 (2017).
- ³⁶C. J. Delker, Y. Zi, C. Yang, and D. B. Janes, “Low-frequency noise contributions from channel and contacts in InAs nanowire transistors,” *IEEE T. Electron Dev.* **60**, 2900–2905 (2013).
- ³⁷M. Petrychuk, I. Zadorozhnyi, Y. Kutovyi, S. Karg, H. Riel, and S. Vitusevich, “Noise spectroscopy to study the 1d electron transport properties in InAs nanowires,” *Nanotechnology* **30**, 305001 (2019).
- ³⁸K.-M. Persson, B. G. Malm, and L.-E. Wernersson, “Surface and core contribution to 1/f-noise in InAs nanowire metal-oxide-semiconductor field-effect transistors,” *Appl. Phys. Lett.* **103**, 033508 (2013).
- ³⁹K.-M. Persson, E. Lind, A. W. Dey, C. Thelander, H. Sjolund, and L.-E. Wernersson, “Low-frequency noise in vertical InAs nanowire FETs,” *IEEE Electr. Device L.* **31**, 428–430 (2010).
- ⁴⁰R. E. Wahl, F. Wang, H. E. Chung, G. R. Kunnen, S. Yip, E. H. Lee, E. Y. B. Pun, G. B. Raupp, D. R. Allee, and J. C. Ho, “Stability and low-frequency noise in InAs NW parallel-array thin-film transistors,” *IEEE Electr. Device L.* **34**, 765–767 (2013).
- ⁴¹C. Volk, J. Schubert, M. Schnee, K. Weis, M. Akabori, K. Sladek, H. Hardtdegen, and Th. Schäpers, “LaLuO₃ as a high-k-gate dielectric for InAs nanowire structures,” *Semicond. Sci. Technol.* **25**, 085001 (2010).
- ⁴²Ö. Gül, D. J. van Woerkom, I. van Weperen, D. Car, S. R. Plissard, E. P. A. M. Bakkers, and L. P. Kouwenhoven, “Towards high mobility InSb nanowire devices,” *Nanotechnology* **26**, 215202 (2015).
- ⁴³B. M. Freeman, J. S. Schoenfeld, and H. Jiang, “Comparison of low frequency charge noise in identically patterned Si/SiO₂ and Si/SiGe quantum dots,” *Appl. Phys. Lett.* **108**, 253108 (2016).
- ⁴⁴L. Petit, J. Boter, H. Eenink, G. Droulers, M. Tagliaferri, R. Li, D. Franke, K. Singh, J. Clarke, R. Schouten, V. Dobrovitski, L. Vandersypen, and M. Veldhorst, “Spin lifetime and charge noise in hot silicon quantum dot qubits,” *Phys. Rev. Lett.* **121**, 076801 (2018).
- ⁴⁵E. J. Connors, J. Nelson, H. Qiao, L. F. Edge, and J. M. Nichol, “Low-frequency charge noise in Si/SiGe quantum dots,” *Phys. Rev. B* **100**, 165305 (2019).
- ⁴⁶S. R. Plissard, D. R. Slapak, M. A. Verheijen, M. Hocevar, G. W. G. Immink, I. van Weperen, S. Nadj-Perge, S. M. Frolov, L. P. Kouwenhoven, and E. P. A. M. Bakkers, “From InSb nanowires to nanocubes: Looking for the sweet spot,” *Nano Lett.* **12**, 1794–1798 (2012).
- ⁴⁷D. Car, J. Wang, M. A. Verheijen, E. P. A. M. Bakkers, and S. R. Plissard, “Rationally designed single-crystalline nanowire networks,” *Adv. Mater.* **26**, 4875–4879 (2014).
- ⁴⁸K. Flöhr, M. Liebmann, K. Sladek, H. Y. Günel, R. Frielinghaus, F. Haas, C. Meyer, H. Hardtdegen, Th. Schäpers, D. Grützmacher, and M. Morgenstern, “Manipulating InAs nanowires with submicrometer precision,” *Rev. Sci. Instrum.* **82**, 113705 (2011).
- ⁴⁹D. B. Suyatin, C. Thelander, M. T. Björk, I. Maximov, and L. Samuelson, “Sulfur passivation for ohmic contact formation to InAs nanowires,” *Nanotechnology* **18**, 105307 (2007).
- ⁵⁰I. Shorubalko, A. Pfund, R. Leturcq, M. T. Borgström, F. Gramm, E. Müller, E. Gini, and K. Ensslin, “Tunable few-electron quantum dots in InAs nanowires,” *Nanotechnology* **18**, 044014 (2007).
- ⁵¹S. Heedt, I. Otto, K. Sladek, H. Hardtdegen, J. Schubert, N. Demarina, H. Lüth, D. Grützmacher, and Th. Schäpers, “Resolving ambiguities in nanowire field-effect transistor characterization,” *Nanoscale* **7**, 18188–18197 (2015).
- ⁵²Q.-T. Do, K. Blekker, I. Regolin, W. Prost, and F.-J. Tegude, “High transconductance MISFET with a single InAs nanowire channel,” *IEEE Electr. Device L.* **28**, 682–684 (2007).
- ⁵³A. F. Young, C. R. Dean, I. Meric, S. Sorgenfrei, H. Ren, K. Watanabe, T. Taniguchi, J. Hone, K. L. Shepard, and P. Kim, “Electronic compressibility of layer-polarized bilayer graphene,” *Phys. Rev. B* **85**, 235458 (2012).
- ⁵⁴A. Schäfer, F. Wendt, S. Mantl, H. Hardtdegen, M. Mikulics, J. Schubert, M. Luysberg, A. Besmehn, G. Niu, and T. Schroeder, “Hexagonal LaLuO₃ as high-k-dielectric,” *J Vac Sci Technol B* **33**, 01A104 (2015).
- ⁵⁵E. Chanrion, D. J. Niegemann, B. Bertrand, C. Spence, B. Jadot, J. Li, P.-A. Mortemousque, L. Hutin, R. Maurand, X. Jehl, M. Sanquer, S. D. Franceschi, C. Bäuerle, F. Balestro, Y.-M. Niquet, M. Vinet, T. Meunier, and M. Urdampilleta, “Charge detection in an array of cmos quantum dots,” (2020), arXiv:2004.01009.
- ⁵⁶T. F. Watson, S. G. J. Philips, E. Kawakami, D. R. Ward, P. Scarlino, M. Veldhorst, D. E. Savage, M. G. Lagally, M. Friesen, S. N. Coppersmith, M. A. Eriksson, and L. M. K. Vandersypen, “A programmable two-qubit quantum processor in silicon,” *Nature* **555**, 633–637 (2018).
- ⁵⁷D. Lynall, S. V. Nair, D. Gutstein, A. Shik, I. G. Savelyev, M. Blumin, and H. E. Ruda, “Surface state dynamics dictating transport in InAs nanowires,” *Nano Lett.* **18**, 1387–1395 (2018).
- ⁵⁸S. A. Dayeh, C. Soci, P. K. L. Yu, E. T. Yu, and D. Wang, “Transport properties of InAs nanowire field effect transistors: The effects of surface states,” *J. Vac. Sci. Technol. B* **25**, 1432 (2007).